scientific reports

Check for updates

OPEN

Effective elimination of Pb (II) cations from waste water and polluted water using siderite magnetic biochar

Saeid Gitipour[1], Mahsa Sanaei[1]✉, Razyeh Lak[2] & Abdolreza Karbassi[1]

Magnetic biochar composites were created by pyrolyzing siderite and sawdust in nitrogen gas (N_2). adsorption was done in a variety of pH and temperature ranges on magnetic biochar. A magnet was used to extract the MB-liquid from each other following 24-hour shaking period. At Iran's Geological Survey, Pb(II) concentration was measured using an ICP (Inductively Coupled Plasma). The adsorption-desorption process was carried out five times in order to evaluate the magnetic biochar's reusability. The Pyrolysis of siderite in order to gain the MB changes its chemical composition and turns into a mixture of hematite, magnetite and maghemite, which imparts magnetism to the biochar and enriches its surface functional groups. The characterizations showed a higher specific surface area and porous structures in the magnetic biochar. An external magnetic field (magnet) was used to easily separate the magnetic biochar suspension because XRD investigation revealed that the primary component of the siderite magnetic biochar absorbent is magnetite, a ferrimagnetic mineral with substantial magnetic characteristics. The magnetic biochar composites' strong adsorption capabilities toward Pb (II) ions were demonstrated by the batch adsorption tests. At pH 5.0 and T = 45 °C, Pb had its highest adsorption capability on magnetic biochar 96.92%. The mesoporous structure of magnetic biochar was indicated by the type IV isotherm. It has been demonstrated that adsorption most closely matches Langmuir's model. Therefore, it can be said that monolayer adsorption has occurred. Biochar's active sites were probably responsible for the fast adsorption process. Kinetics of lead adsorption with MB have been harmonized with pseudo-second order, indicating that the predominant mechanism for Pb adsorption onto magnetic biochar is chemisorption/surface complexation. In summary, magnetic biochar serves as a dual-functional material, adsorbing Pb(II) species and reducing them to less harmful forms, with the added advantage of easy recovery and reuse due to its magnetic properties. This makes it a promising material for the remediation of lead-contaminated environments.

Keywords Adsorption, Magnetic, Biochar, Pb(II), Pyrolysis, Siderite

According to Lu et al. (2017)[1] and Gupta et al. (2011)[2], lead is one of the carcinogenic elements that can seriously harm human health, cause disorders in children, and raise the chance of mortality. Many industries such as mining, textile dyeing, battery manufacturing, metal electroplating, gasoline burning and fertilizer industry release toxic Lead into the environment through wastewater and untreated waste. Therefore, the Pb(II) concentration must be reduced before release. Adsorption is the most frequently used technology because it is inexpensive and effective[3–5]. Biochar usually created as pyrolyzing organic materials in anoxic conditions, which reduces the volume/mass of trash[6]. This is because biochar has a very vast exterior area and negative surface charge[7]. Researches indicate that electrostatic attraction and physiochemical sorption are the ways in which biochar interacts with environmental pollutants. Biochar is a versatile product, but its wide application in wastewater remediation has been hindered by the difficulty of separating it from solutions[8].

Many types of biochars are being used as an adsorbent to remove multiple contaminants, including heavy metals, nutrients and organic compounds from environments.

Biochar has a high specific surface area and a rich porous structure and more over in its surface has oxygen-containing functional groups[9,10]. Biochar can be made from a wide range of low cost carbon containing materials, such as agricultural or forestry waste, animal manure and urban sludge[11]. Studies have showed the

[1]Faculty of environment, University of Tehran, Tehran, Iran. [2]Research Institute for Earth Sciences, Geological Survey and Mineral Exploration of Iran, Tehran, Iran. ✉email: mahsa.sanaei@ut.ac.ir

chemical composition	Fe_2O_3	FeO	SiO_2	Others	loss on ignition
mass fraction(%)	64.50	14.90	9.70	2.60	8.30

Table 1. Chemical composition of siderite.

chemical composition	O	C	H	*N*	S
mass fraction(%)	38.93	37.42	6.04	0.82	0.075

Table 2. Chemical composition of sawdust.

use of biochar in adsorbing metal ions. biochar prepared by the pyrolysis of wood ear mushroom sticks exhibits a high adsorption capacity for Cd^{2+} and $Pb^{[2+}$ [12]. biochar prepared from agricultural waste rice husks through pyrolysis possesses a high specific surface area[13].

According to investigations, lead prefers attract to the exterior of biochars. The magnetic material used to make the magnetic biochar in this study was natural siderite, which was chosen to lower the production costs and encourage the wider usage of natural minerals.

Many researches have been performed on the modification of biochar using various methods for Improving the adsorption capacity of biochar for metal ions and its recyclability, and to increase its specific surface area, the types and quantities of functional groups and to impart magnetism[14,15]. Adding Fe to biochar can increase the specific surface area of biochar and enrich its surface functional groups. it can also regulate the surface charge of biochar, improving its adsorption capacity for metal ions[16,17]. Also, Fe can impart magnetism to biochar, helping its recyclability[18].

Magnetic biochar composites have been widely used to maximize biochar recycling from aqueous solutions. In order to effortlessly extract biochar from an aqueous solution, magnetic biochar was created. Impregnation pyrolysis, co-precipitation, using a reducing agent, and other methods are among the several techniques to create magnetic biochar[19]. Numerous experiments demonstrated magnetic biochar significantly increased adsorption capacity while also achieving the goal of recycling[20].

The process of creating magnetic biochar from iron-bearing materials has been documented in a few publications. Siderite has been reported to convert into magnetic minerals[21] and has been observed that siderite exhibits a range of magnetic properties[22]. siderite has been the subject of researches on the elimination of toxic cations from environmental medium by[23–26].

The magnetic nature of biochar (due to the incorporation of magnetic materials like magnetite or other ferromagnetic substances) allows for easy recovery of the material after use in removing Pb(II) from water or soil. After Pb(II) is adsorbed and reduced, the magnetic properties enable efficient separation and recycling of the biochar, making it a reusable material for environmental remediation[19]. This study synthesized magnetic biochar from siderite and sawdust and examined its adsorption mechanism for Pb(II).

Materials and methods

MB Preparation

The natural siderite (Fe_2O_3 64.50%, FeO 14.90%, SiO_2 9.70%, LOI 8.30%) Table 1, were obtained from Sangan - Khaf, Iran, and sawdust (C 37.42%, O 38.93%, H 6.04%, N 0.82%, S 0.075%) Table 2, from Tehran, Iran. At 80 °C, the sawdust was dried in an oven. To extract particles with the size of 0.150 –0.075 mm, the siderite was sieved. After combining siderite and sawdust of 1:2 weight ratio in DI water, suspension was agitated two hours and after that dried in an oven. The mixture was then put in a biochar reactor in the furnace, which was heated using N_2 for 0.5 h after reaching 550 °C from room temperature. The produced MB granules were removed for characterization and adsorption studies after cooling to room temperature.

The Pyrolysis of siderite in order to gain the MB changes its chemical composition and turns into a mixture of hematite, magnetite (**Eq. 1**) and maghemite, which imparts magnetism to the biochar and enriches its surface functional groups.

$$\text{Pyrolysisofsiderite} : FeCO_3 \rightarrow Fe_3O_4 + CO_2 + CO \quad (1)$$

Batch experiment

To investigate adsorption on MB sample, $PbNO_3$ solution (100 mg/L Pb^{2+} cation) were mixed with 0.1 g of the adsorbent at room temperature (30 °C) in a 100 mL backer. In the studies, NaOH or HCl weak solutions were added if needed to change the pH of the test solutions. A shaker was used to spin the backer holding the adsorbent and adsorbate at 30 rpm. A magnet was used to extract the MB-liquid phases following the 24-hour shaking period. At Iran's Geological Survey, the amount of Pb cation was calculated using an ICP (Inductively Coupled Plasma).

The effect of temperature (15–60 °C) and pH (2–8) on the MB's elimination of Pb(II) was assessed. The adsorption-desorption process was done five cycles to examine the reusability of magnetic biochar. Wet-MB solid was washed with the HCl solution, and the adsorption was then repeated using the cleaned MB.

Characterization

By using a Philips MAGIX PRO XRF-PW2400 X-ray fluorescence spectrometer, the chemical conformation of natural mineral was determined. A Fourier transform infrared spectrometer (FT-IR) (Bruker, WQF-510) was helped to distinguish the structural groups of magnetic biochar. The total content of carbon, nitrogen, oxygen, and hydrogen was obtained using the Eager 300 elemental analyzer (CHN for EA1112). A magnetometer from LBKFB- Kavir Magnetic Co., Kashan, Iran, was used to create the magnetization curve. Dispersive X-ray spectroscopy (EDS) (EDX Oxford UK) and SEM (ZEISS, Germany) scanned the morphology of magnetic biochar. with Cu Kα at 40 mA and 40 kV, an X-ray diffractometer (Bruker, Germany) fitted with a rotation anode was used to examine the mineralogy of magnetic biochar. The (BET) quantified the S_{BET} utilizing N_2 sorption and the TriStar II 1020 equipment.

Results and discussion

Characterizations

In Fig. 1A the FT-IR bands seen at 1100 and 1030 cm^{-1} are for the C-O stretching vibration[27]. The C = O and C = C vibrations are associated with the band at 1545 cm^{-1} [28,29]. bands at 465 and 560 cm^{-1} are for Fe-O stretching vibration Fe_3O_4 [30,31].

The XRD diagram of the pyrolyzed MB is given in Fig. 1B. The XRD diagram indicates that siderite is changed into magnetite (Fe_3O_4) at 500 °C. XRD measurements were used to determine the crystal phase and structural information of the magnetic biochar (Fig. 1B). Based on XRD analysis, it was found that the siderite magnetic biochar absorbent is mainly composed of magnetite, a ferrimagnetic material with significant magnetic properties, that its black colour defines this well. Therefore, separating magnetic biochar suspension with an external magnetic field (magnet) is simple.

The magnetic hysteresis loop of room-temperature magnetic biochar is depicted in Fig. 1C. Magnetic biochar has a better magnetic response, according to specific saturation magnetization. During the adsorption process, magnetic biochar can be readily separated due to its high magnetic susceptibility[32,33].

Analyzing the morphology of magnetic biochar containing Pb(II) and original magnetic biochar was carried out via SEM-EDS. Magnetite was affixed to the sawdust's porous, fibrous structure in Fig. 1E. The EDS results showed that these granular Microparticles were Fe_3O_4. Following Pb(II) adsorption, the magnetic biochar's SEM picture (Fig. 1D) revealed that Microparticles had been deposited on the porous biochar surface.

According to Fig. 2 MB has a IV isotherm, demonstrating the presence of a mesoporous arrangement[34].

Kinetics of adsorption

Adsorption kinetics can demonstrate the rate of adsorption at the interface between solids and solutions[35]. As shown in Fig. 3 Adsorption occurs quickly during the first five hours, and after that, the rate of adsorption gradually increases until equilibrium is attained. The rapid adsorption process is probably caused by magnetic biochar's active sites.

The strong adsorption and precipitation of biochar have been reported to contribute to its high performance in accumulating Pb(II)[36,37]. The rapid adsorption rate is thought to be caused by an abundance of active spots, such as wide exterior area as well as rich pore structure[38].

The kinetic data were used to probe the adsorption procedure in more detail. Table 3 displays the employed sample's adsorption kinetics.

Pseudo-second-order model had a higher R^2 than to the pseudo-first-order model. According to[39], based on kinetics data, pseudo-second-order model, and therefore chemical adsorption is dominating.

Effect of pH

The cations of heavy metals adsorption is frequently greatly influenced by solution pH[40]. this happens because of the ion speciation of heavy metals, chemistry and functional group as well as the surface charge of the adsorbent. To ascertain for impact of medium pH on the MB's efficiency for Pb(II), a pH range of 2 to 8 was chosen. The sorption capacity increased noticeably during pH 2 to 5, as shown in Fig. 4, and subsequently declined as the pH increased to 8.

Figure 5 showed the range of lead species in various pH medium. for pH < 4, Pb^{2+} was the predominant Pb(II) species. Cations of lead, like $Pb(OH)^+$, were detected between pH 4 and 8, whereas anions of lead, like $HPbO_2^-$, and the hydroxide $Pb(OH)_2$ were detected at pH > 8. At high pH values, the quantity of H^+ decreased, which in turn reduced competition and increased the adsorption capacity. The MB surface develops negative sites, which increases the attraction between the MB surface and cations[41]. As the pH rose to 6, Pb(II) may not have been able to diffuse to the porous MB's adsorption sites because to the presence and adsorption of $Pb(OH)^+$[40].

The considerable progress in lead adsorption on MB at pH 2–5 can be attributed to the electrostatic interactions among the positive species of Pb(II) in solution and surface of magnetic biochar with negative charges. Therefore, it is likely that electrostatic interactions will cause the progress in lead adsorption by MB at pH 2-5[42]. Instead, it is more likely the result of Pb(II) species surface complexation/reduction on magnetic biochar[43], and the repulsion between negatively charged magnetic biochar and negative Pb(II) species will cause the decrease in lead collection at pH > 5.

The surface complexation and reduction of Pb(II) species on magnetic biochar involve both adsorption processes and the reduction of lead ions to a less toxic state. Here's a breakdown of what happens: **Surface Complexation**: Magnetic biochar has a large surface area and contains functional groups (like hydroxyl, carboxyl, and amine groups) that can interact with Pb(II) ions. These functional groups facilitate the adsorption of Pb(II) on the surface of the biochar, forming surface complexes. The biochar acts as a sorbent, and Pb(II) ions bind to these surface groups via electrostatic interactions, ligand exchange, or hydrogen bonding. **Reduction of Pb(II) to Pb(0)**: Magnetic biochar, especially if it is impregnated with iron oxide (which is often the case

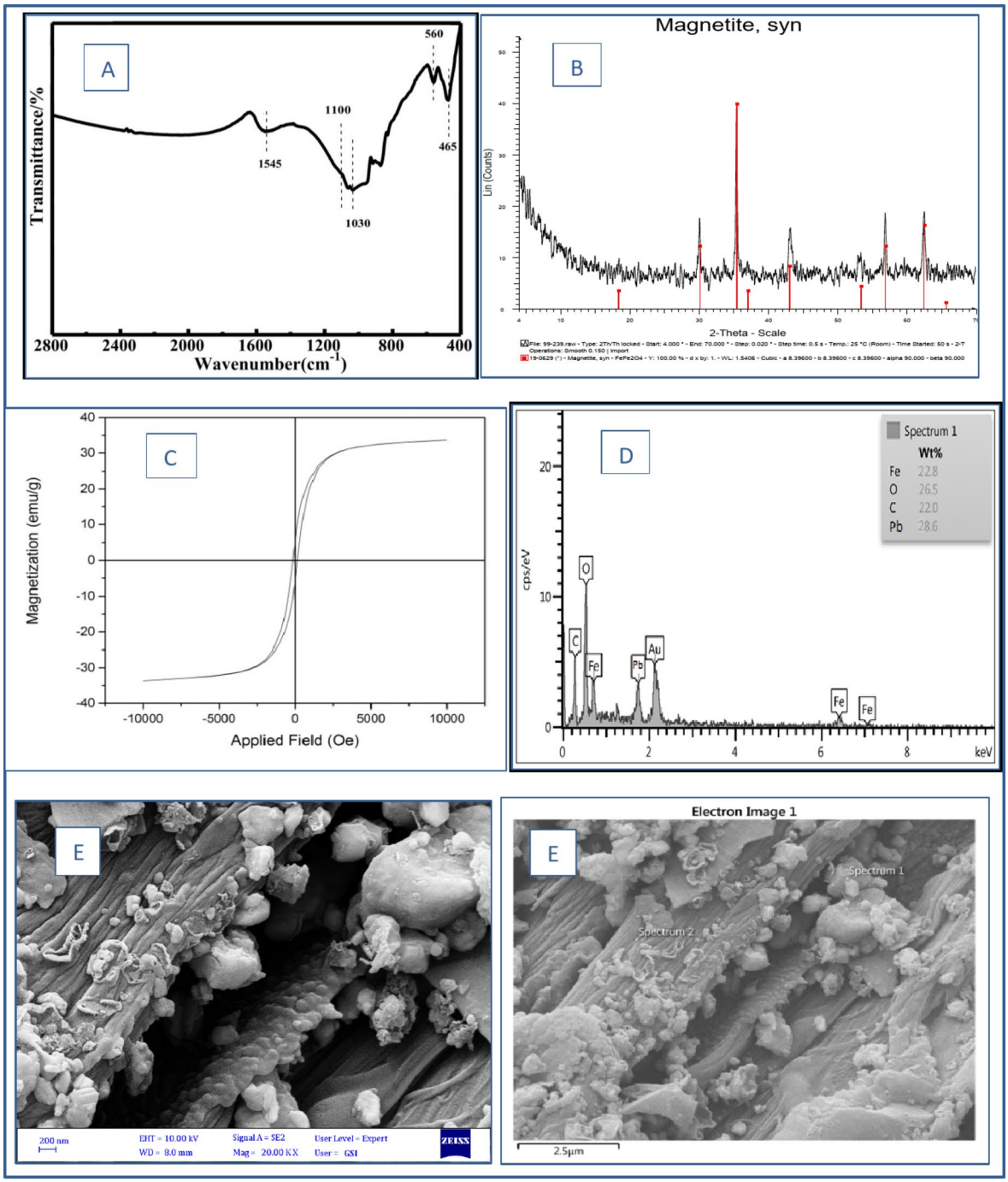

Fig. 1. Magnetic biochar's characteristics. A: FTIR spectra; B: XRD patterns; C: magnetic hysteresis loops; D & E: SEM images.

in "magnetic biochar"), has the potential to reduce Pb(II) to Pb(0) (elemental lead). This happens due to the presence of iron or iron oxide particles on the biochar surface, which can act as reducing agents. The iron species can donate electrons to Pb(II), reducing it to Pb(0), which is less soluble and less mobile in the environment. This transformation is a key part of the detoxification process, as Pb(0) is much less toxic than its ionic form. In summary, magnetic biochar serves as a dual-functional material, adsorbing Pb(II) species and reducing them to less harmful forms.

Effect of temperature

Temperature effects revealed that Pb(II) was most able to adsorb onto magnetic biochar at 45 °C and least at 15 °C (Fig. 6). The data suggests that the ability of magnetic biochar to adsorb Pb(II) is temperature-dependent. This temperature dependency could be due to several factors: **Increased Kinetic Energy**: Higher temperatures

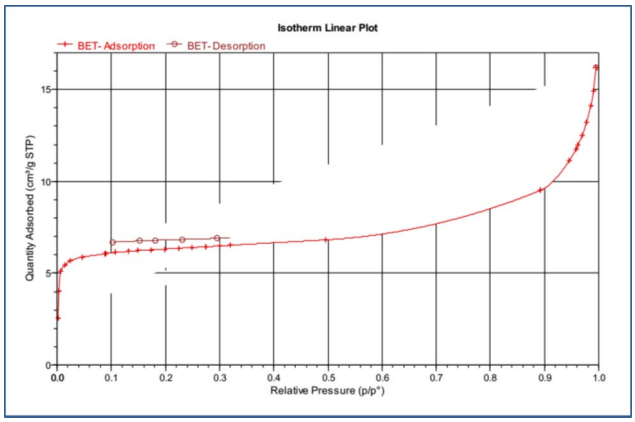

Fig. 2. N_2-adsorption-desorption isotherm.

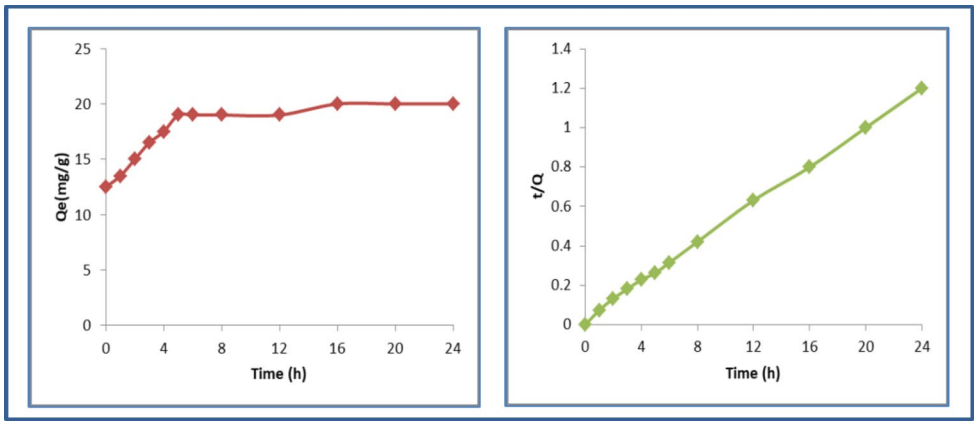

Fig. 3. left: kinetics of Lead on magnetic biochar, right: pseudo-second-order model.

Sample	pseudo-first-order			pseudo-second-order		
MB	q_{e1} ($mg \cdot g^{-1}$)	K_1 (min^{-1})	R^2	q_{e2} ($mg \cdot g^{-1}$)	K_2 ($g \cdot (mg \cdot min)^{-1}$)	R^2
	8.32	0.0051	0.8101	16.69	0.0032	0.9483

Table 3. Kinetics for lead adsorption on MB.

might increase the kinetic energy of both the Pb(II) ions and the adsorption sites on the magnetic biochar, leading to a greater interaction between the two. **Enhanced Diffusion**: As temperature increases, the diffusion rate of Pb(II) ions into the pores of the biochar may improve, leading to better adsorption. **Changes in Surface Chemistry**: The surface properties of the biochar (such as charge, surface area, and functional groups) may be affected by temperature, potentially making it more favorable for Pb(II) binding at higher temperatures.

On the other hand, at lower temperatures (such as 15 °C), these processes might be slower or less efficient, leading to reduced adsorption.

The drop in Pb(II) adsorption from 45 °C to 60 °C could be due to several factors that influence the efficiency of adsorption at higher temperatures. Like Desorption at Higher Temperatures, Changes in Surface Properties, Increased Viscosity of Water or Solution, Ion Pairing or Precipitation and Saturation of Adsorption Sites. In summary, while lower temperatures (like 15 °C) result in less efficient adsorption, higher temperatures (such as 45 °C) likely provide the optimal conditions for Pb(II) adsorption. However, at temperatures above 45 °C, factors like desorption, surface changes, and ion interactions might cause a decrease in adsorption efficiency.

Adsorption isotherm

The Freundlich and Langmuir models were used to simulate the Pb(II) adsorption isotherm on the MB. According to[39], the Langmuir model postulates monolayer adsorption on a homogenous surface with a constant

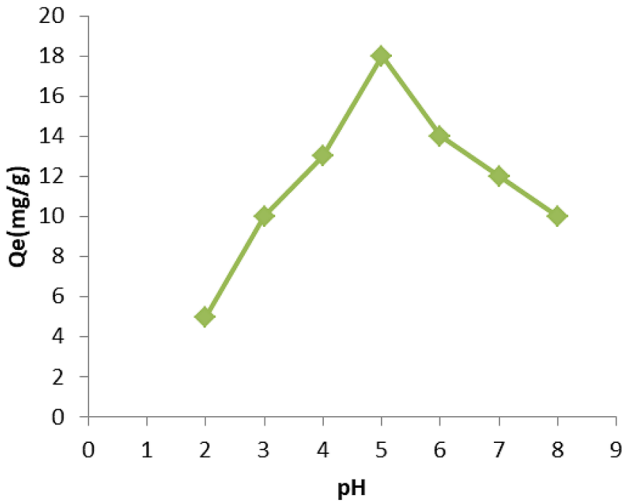

Fig. 4. Effect of pH on MB adsorption.

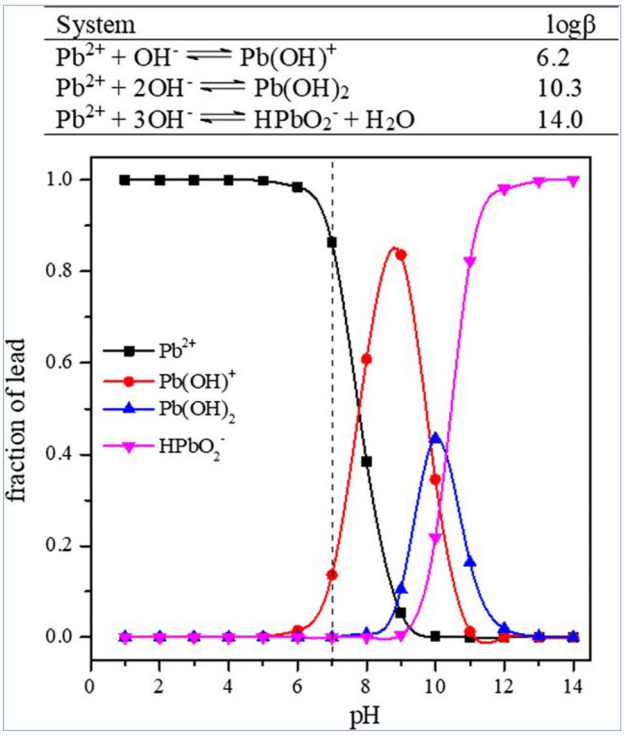

Fig. 5. Lead species Distribution in different pH.

number of adsorption sites, meaning that there is no interaction between adsorbed molecules. However, a multilayer adsorption on a heterogeneous adsorbent surface is assumed by the Freundlich model.

Langmuir and Freundlich models were used to match the experimental data[44]. The outcome demonstrated that the superior R^2 of the Langmuir equation ($R^2 > 0.95$) overfitted the Freundlich model, suggesting that Pb(II) adsorption on MB takes place with Single layer coating.

Table 4 displays Freundlich and Langmuir models characteristics. Figure 7 displays the Pb(II) adsorption isotherm in the Langmuir model on the MB.

For practical applications, magnetic biochar's reusability is essential. Pb(II) has been extensively removed from adsorbents using acid elution. According to Fig. 8, the amount of lead adsorbed on the MB reduced after five cycles washing with the weak acidic desorption procedure. The small decrease in adsorption quantity was explained by solid loss in solution and incomplete Pb(II) desorption on the magnetic biochar surface. Pb(II) from desorption solutions can also be pre-concentrated and immobilized[45].

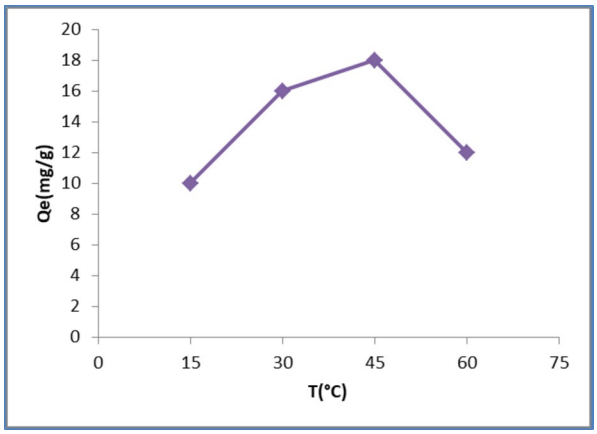

Fig. 6. Effect of temperature on magnetic biochar adsorption.

Sample		Langmuir			Freundlich	
	q_m ($mg \cdot g^{-1}$)	K_L ($L \cdot mg^{-1}$)	R^2	K_F ($mg \cdot g^{-1}$)	1/n	R^2
MB	18.32	0.13	0.9525	3.05	0.025	0.8483

Table 4. Parameters for Langmuir and Freundlich models.

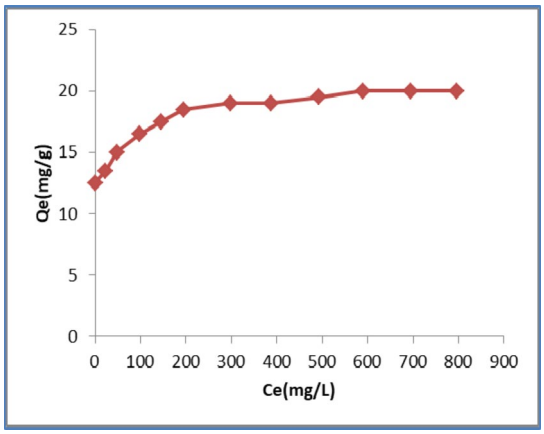

Fig. 7. Adsorption isotherm.

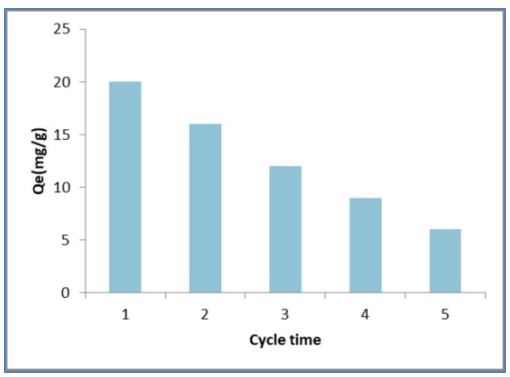

Fig. 8. cycle experiments of Pb(II) adsorption on MB.

Conclusions

When Pb(II) was exposed to magnetic biochar at pH 5.0 and T = 45 °C, its maximum adsorption capability was achieved with 96.92%. For comparison The Pb (II) adsorption onto biochar[46] was spontaneous in the specified temperature range (298–318 K) and the process was exothermic. Simultaneously, the optimal conditions were a pH of 5, under which the maximum predicted Pb(II) removal efficiency was 91.52%.

Our adsorbents were created via heating siderite and sawdust in biochar reactor conditions. This is an economically, environmentally and effective process. The performance of the adsorption was greatly enhanced by the pyrolysis. For this occurrence, an increase in surface area should be taken into account. Co-pyrolysis increased the adsorbent's magnetism, which is advantageous for using a magnet to separate solids from liquids.

In summary, magnetic biochar serves as a dual-functional material, adsorbing Pb(II) species and reducing them to less harmful forms, with the added advantage of easy recovery and reuse due to its magnetic properties. This makes it a promising material for the remediation of lead-contaminated environments.

The adsorption tests showed that Pb(II) from environmental medium could be adsorbed with magnetic biochar composites, and that the MB-Pb residue could be simply extracted from the suspension medium with a simple magnet.

It has been proven that magnetic biochar is a good sorbent for remediation of lead-contaminated environments and has a good adsorption capacity for Pb(II). For Pb(II) environmental remediation, MB adsorbent is suggested to be employed because of its straightforward synthesis process, inexpensive cost, ease of separation, good efficiency and environmental friendliness.

These findings also showed that magnetic biochar might be a viable substitute for adsorbent in a variety of environmental applications, lowering the danger of Pb(II) contamination and other heavy metal ions, by variation and optimization in magnetic biochar synthesis in future researches.

Data availability

The datasets used and/or analysed during the current study available from the corresponding author on reasonable request.

Received: 23 January 2025; Accepted: 25 February 2025
Published online: 06 March 2025

References

1. Lu, X. et al. Transformation of hazardous lead into lead ferrite ceramics: crystal structures and their role in lead leaching. *J. Hazard. Mater.* **336**, 139–145. https://doi.org/10.1016/j.jhazmat.2017.04.061 (2017).
2. Gupta, V. K., Agarwal, S. & Saleh, T. A. Synthesis and characterization of alumina-coated carbon nanotubes and their application for lead removal. *J. Hazard. Mater.* **185**, 17–23. https://doi.org/10.1016/j.jhazmat.2010.08.053 (2011).
3. Bairagi, H., Khan, M. M. R., Ray, L. & Guha, A. K. Adsorption profile of lead on Aspergillus versicolor: a mechanistic probing. *J. Hazard. Mater.* **186**, 756–764. https://doi.org/10.1016/j.jhazmat.2010.11.064 (2011).
4. Luo, J. et al. Tuning Pb (II) adsorption from aqueous solutions on ultrathin iron oxychloride (FeOCl) nanosheets, Environmental science & technology. 53, 2075–2085. https://pubs.acs.org/doi/full/ (2019). https://doi.org/10.1021/acs.est.8b07027
5. Godiya, C. B., Cheng, X., Li, D., Chen, Z. & Lu, X. Carboxymethyl cellulose/polyacrylamide composite hydrogel for cascaded treatment/reuse of heavy metal ions in wastewater. *J. Hazard. Mater.* **364**, 28–38. https://doi.org/10.1016/j.jhazmat.2018.09.076 (2019).
6. Chen, B. & Chen, Z. Sorption of naphthalene and 1-naphthol by biochars of orange peels with different pyrolytic temperatures. *Chemosphere* **76**, 127–133. https://doi.org/10.1016/j.chemosphere.2009.02.004 (2009).
7. Zhang, X. et al. Removal of uranium (VI) from aqueous solutions by magnetic schiff base: kinetic and thermodynamic investigation. *Chem. Eng. J.* **198**, 412–419. https://doi.org/10.1016/j.cej.2012.05.090 (2012).
8. Jung, K. W., Lee, S. & Lee, Y. J. Synthesis of novel magnesium ferrite (MgFe2O4)/biochar magnetic composites and its adsorption behavior for phosphate in aqueous solutions. *Bioresour. Technol.* **245**, 751–759. https://doi.org/10.1016/j.biortech.2017.09.035 (2017).
9. Leng, L. et al. Engineering Biochar from biomass pyrolysis for effective adsorption of heavy metal: an innovative machine learning approach. *Sep. Purif. Technol.* **131592** https://doi.org/10.1016/j.seppur.2025.131592 (2025).
10. Zhou, R., Zhang, M. & Shao, S. Optimization of target Biochar for the adsorption of target heavy metal ion. *Sci. Rep.* **12** (1), 13662. https://doi.org/10.1038/s41598-022-17901-w (2022).
11. Ji, J., Yuan, X., Zhao, Y., Jiang, L. & Wang, H. Mechanistic insights of removing pollutant in adsorption and advanced oxidation processes by sludge biochar. Journal of Hazardous Materials, 430, 128375, (2022). https://doi.org/10.1016/j.jhazmat.2022.128375 (2022).
12. Ji, Y., Zheng, N., An, Q., Sun, S., Wang, S., Li, X., … Zhang, W. The effect of carbonization temperature on the capacity and mechanisms of Cd (II)-Pb (II) mix-ions adsorption by wood ear mushroom sticks derived biochar. Ecotoxicology and Environmental Safety,239, 113646. https://doi.org/10.1016/j.ecoenv.2022.113646 (2022).
13. Li, Z., Su, Q., Xiang, L., Yuan, Y. & Tu, S. Effect of pyrolysis temperature on the sorption of cd (II) and se (IV) by rice husk Biochar. *Plants* **11** (23), 3234. https://doi.org/10.3390/plants11233234 (2022).
14. Zhang, H., Li, R. & Zhang, Z. A versatile EDTA and Chitosan bi-functionalized magnetic bamboo Biochar for simultaneous removal of Methyl orange and heavy metals from complex wastewater. *Environ. Pollut.* **293**, 118517. https://doi.org/10.1016/j.envpol.2021.118517 (2022).
15. Xu, Y. et al. Study on efficient adsorption mechanism of Pb2 + by magnetic coconut Biochar. *Int. J. Mol. Sci.* **23** (22), 14053. https://doi.org/10.3390/ijms232214053 (2022).
16. Yang, S. et al. Insights into remediation of cadmium and lead contaminated-soil by Fe-Mn modified Biochar. *J. Environ. Chem. Eng.* **12** (3), 112771. https://doi.org/10.1016/j.jece.2024.112771 (2024).
17. Hu, S., Liu, C., Bu, H., Chen, M. & Fei, Y. H. Efficient reduction and adsorption of cr (VI) using FeCl3-modified Biochar: synergistic roles of persistent free radicals and Fe (II). *J. Environ. Sci.* **137**, 626–638. https://doi.org/10.1016/j.jes.2023.03.011 (2024).
18. Chen, Q., Zhang, Y., Xia, H., Liu, R. & Wang, H. Fabrication of two novel amino-functionalized and starch-coated CuFe2O4-modified magnetic Biochar composites and their application in removing Pb2 + and Cd2 + from wastewater. *Int. J. Biol. Macromol.* **258**, 128973. https://doi.org/10.1016/j.ijbiomac.2023.128973 (2024).
19. Li, M., Liu, H., Chen, T., Dong, C. & Sun, Y. Synthesis of magnetic Biochar composites for enhanced uranium (VI) adsorption. *Sci. Total Environ.* **651**, 1020–1028. https://doi.org/10.1016/j.scitotenv.2018.09.259 (2019).

20. Han, Y., Cao, X., Ouyang, X., Sohi, S. P. & Chen, J. Adsorption kinetics of magnetic Biochar derived from peanut hull on removal of cr (VI) from aqueous solution: effects of production conditions and particle size. *Chemosphere* **145**, 336–341. https://doi.org/10.1016/j.chemosphere.2015.11.050 (2016).
21. Xing, B. et al. Removal of phosphate from aqueous solution by activated siderite ore: preparation, performance and mechanism. *J. Taiwan Inst. Chem. Eng.* **80**, 875–882. https://doi.org/10.1016/j.jtice.2017.07.016 (2017).
22. Li, M. et al. Spectroscopic and modeling investigation of Eu (III)/U (VI) sorption on nanomagnetite from aqueous solutions. *ACS Sustain. Chem. Eng.* **5**, 5493–5502. https://doi.org/10.1021/acssuschemeng.7b00829 (2017).
23. Guo, H., Stüben, D., Berner, Z. & Kramar, U. Adsorption of arsenic species from water using activated siderite–hematite column filters. *J. Hazard. Mater.* **151** (2–3), 628–635. https://doi.org/10.1016/j.jhazmat.2007.06.035 (2008).
24. Guo, H., Stüben, D. & Berner, Z. Adsorption of arsenic (III) and arsenic (V) from groundwater using natural siderite as the adsorbent. *J. Colloid Interface Sci.* **315** (1), 47–53. https://doi.org/10.1016/j.jcis.2007.06.035 (2007).
25. Li, M., Liu, H., Chen, T. & Lin, W. Nano-hematite prepared by activation of natural siderite and its performance on immobilization of Eu (III). *Appl. Geochem.* **84**, 154–161. https://doi.org/10.1016/j.apgeochem.2017.06.010 (2017).
26. Zhang, Z., Liu, H., Lu, P., Chen, T. & Ma, W. Nanostructured α-Fe2O3 derived from siderite as an effective hg (II) adsorbent: performance and mechanism. *Appl. Geochem.* **96**, 92–99. https://doi.org/10.1016/j.apgeochem.2018.06.016 (2018).
27. Wang, B., Jiang, Y. S., Li, F. Y. & Yang, D. Y. Preparation of Biochar by simultaneous carbonization, magnetization and activation for Norfloxacin removal in water. *Bioresour. Technol.* **233**, 159–165. https://doi.org/10.1016/j.biortech.2017.02.103 (2017).
28. Zong, P. et al. Synthesis and application of magnetic graphene/iron oxides composite for the removal of U (VI) from aqueous solutions. *Chem. Eng. J.* **220**, 45–52. https://doi.org/10.1016/j.cej.2013.01.038 (2013).
29. Qu, J., Wang, S., Li, Z., Wei, S., Bi, F., Yan, S., … Zhang, Y. Highly efficient recovery of phosphate from water using cerium carbonate hydroxide-decorated magnetic biochar:a slow-release phosphate fertilizer for agricultural reuse. ACS ES&T Engineering,4(12), 3045–3056, https://doi.org/10.1021/acsestengg.4c00407 (2024).
30. Hoseini, S. J., Nasrabadi, H., Azizi, M., Beni, A. S. & Khalifeh, R. Fe3O4 nanoparticles as an efficient and magnetically recoverable catalyst for Friedel–Crafts acylation reaction in solvent-free conditions. *Synth. Commun.* **43**, 1683–1691. https://doi.org/10.1080/00397911.2012.663048 (2013).
31. Shan, C., Ma, Z. & Tong, M. Efficient removal of trace antimony (III) through adsorption by hematite modified magnetic nanoparticles. *J. Hazard. Mater.* **268**, 229–236. https://doi.org/10.1016/j.jhazmat.2014.01.020 (2014).
32. Jin, Z., Wang, X., Sun, Y., Ai, Y. & Wang, X. Adsorption of 4-n-nonylphenol and bisphenol-A on magnetic reduced graphene oxides: a combined experimental and theoretical studies. *Environ. Sci. Technol.* **49** (15), 9168–9175. https://doi.org/10.1021/acs.est.5b02022 (2015).
33. Tripathi, A., Melo, J. S. & D'Souza, S. F. Uranium (VI) recovery from aqueous medium using novel floating macroporous alginate-agarose-magnetite Cryobeads. *J. Hazard. Mater.* **246**, 87–95. https://doi.org/10.1016/j.jhazmat.2012.12.002 (2013).
34. Yu, M. et al. Synthesis of high-performance magnetic Biochar for adsorption of Ni2 + and Co2 + from spent lithium-ion battery effluent. *J. Hazard. Mater. Adv.* **100627** https://doi.org/10.1016/j.hazadv.2025.100627 (2025).
35. Qu, J., Li, Y., Bi, F., Liu, X., Dong, Z., Fan, H., … Zhang, Y. Smooth vetch (Vicia villosa var.) coupled with ball-milled composite mineral derived from shell powder and Phosphate rock for remediation of Cadmium-polluted farmland: Insights into synergetic mechanisms. ACS ES&T Engineering, 4(8), 2054–2067, https://doi.org/10.1021/acsestengg.4c00177 (2024).
36. Zhang, J. et al. Sludge-based Biochar activation to enhance Pb (II) adsorption. *Fuel* **252**, 101–108. https://doi.org/10.1016/j.fuel.2019.04.096 (2019).
37. Ding, W., Dong, X., Ime, I. M., Gao, B. & Ma, L. Q. Pyrolytic temperatures impact lead sorption mechanisms by Bagasse biochars. *Chemosphere* **105**, 68–74. https://doi.org/10.1016/j.chemosphere.2013.12.042 (2014).
38. Naushad, M., ALOthman, Z. A., Awual, M. R., Alam, M. M. & Eldesoky, G. E. Adsorption kinetics, isotherms, and thermodynamic studies for the adsorption of Pb^{2+} and hg^{2+} metal ions from aqueous medium using Ti (IV) Iodovanadate cation exchanger. *Ionics* **21**, 2237–2245. https://doi.org/10.1007/s11581-015-1401-7 (2015).
39. Ifthikar, J. et al. Highly efficient lead distribution by magnetic sewage sludge Biochar: sorption mechanisms and bench applications. *Bioresour. Technol.* **238**, 399–406. https://doi.org/10.1016/j.biortech.2017.03.133 (2017).
40. Kim, S. A. et al. Removal of Pb (II) from aqueous solution by a zeolite–nanoscale zero-valent iron composite. *Chem. Eng. J.* **217**, 54–60. https://doi.org/10.1016/j.cej.2012.11.097 (2013).
41. Shahat, A. et al. Large-pore diameter nano-adsorbent and its application for rapid lead (II) detection and removal from aqueous media. *Chem. Eng. J.* **273**, 286–295. https://doi.org/10.1016/j.cej.2015.03.073 (2015).
42. Sun, Y. et al. Adsorption of U (VI) on sericite in the presence of Bacillus subtilis: A combined batch, Exafs and modeling techniques. 51–65, (2016). https://doi.org/10.1016/j.gca.2016.02.012
43. Wei, S., Tao, Y., Ma, M., Tong, W., Bi, F., Wang, L., … Zhang, Y. One-step microwave-assisted synthesis of MgO-modified magnetic biochar for enhanced removal of lead and phosphate from wastewater: Performance and mechanisms. Separation and Purification Technology,354, 128936, https://doi.org/10.1016/j.seppur.2024.128936 (2025).
44. Phuengprasop, T., Sittiwong, J. & Unob, F. Removal of heavy metal ions by iron oxide coated sewage sludge. *J. Hazard. Mater.* **186**, 502–507. https://doi.org/10.1016/j.jhazmat.2010.11.065 (2011).
45. Amiri-Yazani, T., Zare-Dorabei, R., Rabbani, M. & Mollahosseini, A. Highly efficient ultrasonic-assisted pre-concentration and simultaneous determination of trace amounts of Pb (II) and cd (II) ions using modified magnetic natural clinoptilolite zeolite: response surface methodology. *Microchem. J.* **146**, 498–508. https://doi.org/10.1016/j.microc.2019.01.050 (2019).
46. Yang, W., Lu, C., Liang, B., Yin, C., Lei, G., Wang, B., … Jing, Y. Removal of Pb(II) from aqueous solution and adsorption kinetics of corn stalk biochar. Separations.10(8), 438. https://doi.org/10.3390/separations10080438 (2023).

Acknowledgements

I wish to thank the Geological Survey of Iran (GSI) for their support in every aspect to finalize the present work.

Author contributions

M.S. did the experiments M.S. wrote the main manuscript textM.S. prepared figuresR.L. supervised during the experiments and resources. S.G and A.R. K. supervised during the whole project.

Funding

No Funding.

Declarations

Competing interests

The authors declare no competing interests.

Conflict of interest
On behalf of all authors, the corresponding author states that there are no competing interests.

Author contributions statement
M.S. conceived the experiment(s), M.S. and R.L. conducted the experiment(s), M.S. and R.L. analysed the results. All authors reviewed the manuscript.

Additional information
Correspondence and requests for materials should be addressed to M.S.

Reprints and permissions information is available at www.nature.com/reprints.

Publisher's note Springer Nature remains neutral with regard to jurisdictional claims in published maps and institutional affiliations.